ASTRONOMY & ASTROPHYSICS
SUPPLEMENT SERIES

Astron. Astrophys. Suppl. Ser. **130**, 561–566 (1998)

Isokinetic patch measurements on the edge of the Moon

A. Ghedina, R. Ragazzoni, and A. Baruffolo

Astronomical Observatory of Padova, vicolo dell'Osservatorio 5, I–35122 Padova, Italy
e-mail: ghedina@astras.pd.astro.it; ragazzoni@pd.astro.it; baruffolo@pd.astro.it

Received July 21; accepted December 24, 1997

Abstract. By imaging the edge of the Moon we have tested a seeing monitor able to evaluate the isokinetic patch size. These measurements have a relevant interest because of several Laser Guide Star (LGS) tilt recovery schemes that have been proposed. In our approach the edge of the Moon mimics a LGS as seen far from the laser projector. The conceptual design of the instrument, the data reduction techniques and the preliminary results obtained at the Asiago Astronomical Observatory are given. Because, as a by product, the instrument is able to evaluate r_0, a comparison with seeing data collected at the 1.82 m telescope of Cima Ekar during the three nights test of the described instrument is also given.

Key words: Moon — instrumentation: adaptive optics

1. Introduction

The isokinetic patch size can be defined as the characteristic angular size where the tilt induced by atmospherical perturbation becomes decorrelated. In order to obtain an optimal correction with an Adaptive Optics system it is necessary to have a bright reference source within the isoplanatic patch. Projecting a Laser Guide Star (LGS in the following) inside of the isoplanatic patch, as proposed by Foy and Labeyrie (1985), is convenient when correcting the higher order terms of the perturbation, but it must be considered that tilt alone represents nearly 87% of the wavefront phase variance (Noll 1976). The feasibility of using a LGS as a reference source, apart from the problem of focal anisoplanatism (Tallon & Foy 1990), is fundamentally constrained by the tilt indetermination problem (Pilkington 1987). As regard to the latter, it is known that due to reciprocity in the upward and downward path of the projected laser, the tilt of an LGS is almost completely compensated, at least when the telescope has the same diameter of the projector.

Send offprint requests to: R. Ragazzoni

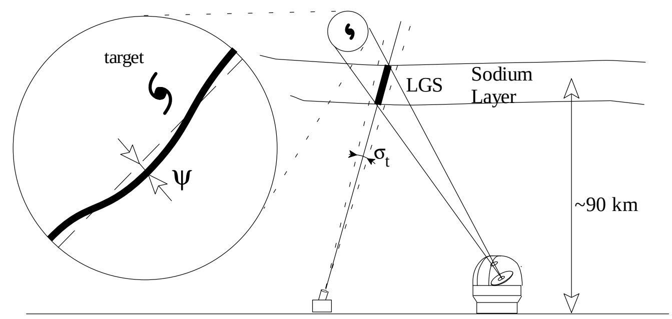

Fig. 1. The effect of the atmospheric turbulence on the propagation of an LGS

A Natural Guide Star (NGS) could be used as a further reference source to recover the absolute tilt of the LGS (Rigaut & Gendron 1992) but, from the scientific point of view, there is a major drawback due to the limited sky coverage, and for this reason it is not a useful technique.

Several other techniques have been proposed recently to recover the tilt of LGSs: (Foy et al. 1992; Foy et al. 1995; Belenk'ii 1994, 1995, 1996; Ragazzoni et al. 1995; Ragazzoni & Marchetti 1996; Ragazzoni 1996a,b, 1997). Some of these take advantage of the loss of reciprocity when the LGS is observed from a point of the earth's surface different from where it is projected.

Two different kinds of tilt perturbation, introduced into the LGS path by the atmospheric turbulence, can be recognized when observing the elongated projection in the sky of the laser.

The first one can be seen as a random and rigid motion of the elongated LGS: it is a jittering effect due to the turbulence met by the LGS in its way up to the sodium layer.

The other perturbation is a deviation ψ from a straight propagation of the laser beacon (see Fig. 1). The elongated LGS is corrugated by the atmospheric turbulence during its propagation from the sodium layer to the observer; in fact the laser stripe spans over a distance which is larger than the typical coherence length of the atmospheric perturbations. The light coming from different portions of the

LGS is then affected in different manners by the turbulence it has to go through: the LGS is thus seen as a line of non coherent sources (where "non coherent" should be intended here as characterized by non coherent movements) and whose mutual distance is determined by the size of the isokinetic patch.

Both tilt perturbations, either of the whole strip or of one single part of the LGS within the same isokinetic patch, are characterized by a Gaussian distribution around a mean position, and a RMS, $\sigma_{\rm t}$, given by:

$$\sigma_{\rm t} \approx k\frac{\lambda}{D}\left(\frac{D}{r_0}\right)^{5/6} \tag{1}$$

in which the "constant" $k \approx 0.4$ has different values depending on the authors, from $k = 0.413$ (Acton 1995) to $k = 0.427$ (Olivier et al. 1993). D is the diameter either of the laser projector or of the observing telescope.

From a theoretical point of view the size of the isokinetic patch can be approximated with the following equation:

$$\theta_0 \approx 0.3\frac{D}{\tilde{h}}\ [\mathrm{rad}], \tag{2}$$

where $\tilde{h}$ is the typical height of the perturbing layer in the atmosphere.

Both perturbations are observed only perpendicularly to the projection in the sky of the laser (if it is a CW laser) and for this reason at least two elongated LGS are needed to recover a bidimensional perturbation.

As far as the isokinetic patch is concerned, the values one can find in the literature are based upon observations of small star clusters or speckle interferometry of double stars (McAlister 1976) and are summarized in Table 1.

Table 1. [1]McClure et al. (1991); [2]Sivaramakrishnan et al. (1995); [3]Christou et al. (1995); [4]Weigelt (1979)

N. of stars	Min dist.	Max dist.	Typ. $\tilde{h}$ [m]	Ref.
12	$\approx 15''$	$\approx 90''$	≈ 3000	1
6	$\approx 38''$	$\approx 55''$	≈ 3800	2
4	$1\farcs27$	$15\farcs50$	< 5800	3
2	$\approx 20''$	$\approx 22''$	> 3000	4

The centroid motion of the stars is measured compared to a reference star and the information one can get about tilt are discretized in space, though continuous in time, because it is not possible to sample the atmospheric turbulence which is not passed through by the light of the stars. By the way, to our knoweledge, the only published attempt to estimate the isokinetic patch size from a continuous target, in this case the edge of the Sun, is by Kallistratova (1966). However, probably due to dominant ground layers occuring during daylight observations only a lower limit of $20''$ is reported.

It is to be pointed out that knowing the size of the isokinetic patch is very interesting for several reasons. Considering the auxiliary telescopes technique (Ragazzoni et al. 1995) for example, it is clear that the position and the speed of the auxiliary telescopes depend upon the size of the isokinetic patch around the NGS used to overcome the tilt problem. In fact the apparent position of the LGS must intersect both the isokinetic patch of the target and of the NGS to obtain the proper tilt of the target alone. The isokinetic patch is a constraint also on the number of photons that can be collected by the auxiliary telescope: this is due to the fact that, of the whole elongated LGS, only that portion which is within the same isokinetic patch is useful to take differential tilt measurements. As a consequence, also the power of the projected laser and the diameter of the auxiliary telescopes have to be established from the typical isokinetic patch size at the observatory site.

In another tilt determination technique (Ragazzoni 1997) the same statements as above are true for the auxiliary projectors.

Finally one can consider two of the other proposed techniques (Belen'kii 1994; Ragazzoni 1995) in which increasing the field of view of the observer allows to consider more isokinetic patches at the same time. As a consequence, while the perturbation introduced during the upward path of the LGS remains the same, it is possible to separate with higher accuracy the contribution of the two perturbations to the tilt effect.

In this paper by imaging a portion of the edge of the Moon we describe the measurements of characteristical parameters of the atmospheric turbulence pretending to observe an elongated LGS.

Even though the edge of the Moon is not straight (see Fig. 2) the curvature of the surface has a negligible effect in the determination of the correlation between the perturbations because the interesting part of the observed portion is less than 1 arcmin wide.
It can also be understood that the adopted method of measuring the differential perturbation between the edges of the Moon allows one to ignore both the curvature and any feature of the lunar limb.

2. The instrument concept

The telescope that has been used in the experiment is a Meade 2080 Schmidt–Cassegrain F/10 with a focal length of $f = 2032$ mm. The images of the Moon were captured with a PXL211 CCD: it uses a Texas Instruments TC211 CCD, 165×192 rows by columns, with a pixel size of 16 μm$\times$13.75 μm. When the CCD is mounted at the focus of the telescope the scale of the system is of 1.6 by 1.4 arcsecs per pixel perpendicularly to the edge of the Moon and along it, respectively.

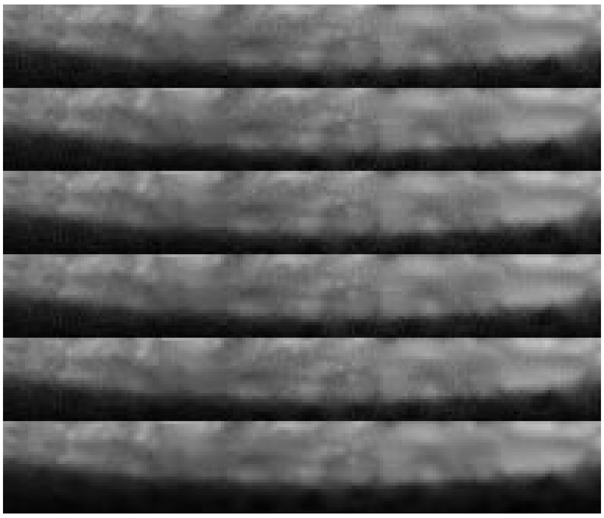

Fig. 2. An image with 6 frames of the edge of the Moon obtained without the anamorphic relay

It is also well known that in the CCD the matrix of pixels is sent, one row at a time, to the serial register where the pixels are read sequentially. While the process of shifting each row or each pixel is very fast (of the order of 10^{-7} s) in our low cost interface there is a bottleneck due to the A/D conversion of each pixel.
In order to freeze the effect of the atmosphere on the images of the lunar edge, it is necessary to overcome this limit. We adopted the approach of using a frame transfer technique so that more images of the Moon are collected in the same frame and it is possible to have an equivalent frame rate of roughly 20 Hz. The edge of the Moon is imaged in n of the lines which are on the side of the CCD opposite to the serial register. Here n is the number of rows of the CCD over the number of images of the Moon that we want to have on the same frame, s.
After the first exposure (of the order of $t = 50$ msec), the image of the edge is shifted of n lines, which are then discarded. After s exposures, on the matrix there are s different images of the edge of the Moon (Fig. 2) and the pixels can now be converted into digital data.

In addition, for some of the measurements performed in this experiment, an anamorphic optical relay is inserted between the focus of a the Schmidt–Cassegrain telescope and the CCD.
It is known (Laikin 1973) that in the CinemaScope system, using a conventional 35 mm cinematographic film, the image projected is twice wider than its height. This is achieved by placing an anamorphic objective after the objective of the projector. The anamorphic objective is an afocal optical system usually made of cylindrical lenses: it shortens the focal length of the main objective in one nodal plane while leaving unchanged the focal length in the complementar direction. To avoid any problem of astigmatism, due to the presence of cylindrical lenses, the anamorphic objective should work in collimated light.

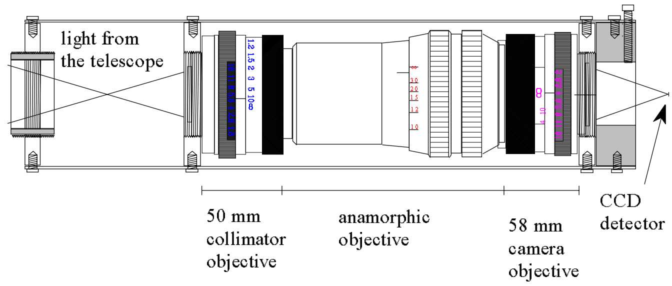

Fig. 3. The anamorphic relay used in this experiment. From left to right one can see the collimator, the anamorphic objective and the second camera objective. The light from the telescope arrives from the left side while on the other side it goes to the CCD

The anamorphic relay used in this experiment is made of a cylindrical tube (see Fig. 3) in which a 50 mm camera objective (collimator), the anamorphic objective and another 58 mm camera objective take place. With the anamorphic relay a double portion of the edge of the Moon (if the anamorphic relay is properly oriented) can be imaged on the CCD: inversely, turning the anamorphic objective upside down and rotating it around its axis of 90°, the perturbation observed on the edge of the Moon can be expanded of a factor of 2.
We wish to point out that we have used very simple and low cost instrumentation which is nevertheless able to demonstrate with reasonable confidence the feasibility of our technique.

3. Data reduction

The following step is the determination of the position of the lunar edge in each image and then the correlation between the images of the same frame. The edge is found column by column introducing a coordinate, x, and a function, $I(x)$, proportional to the intensity of the pixels in that column (see Fig. 4(above)). It is assumed that the edge of the Moon produces an intensity leap higher than any other feature in the image (except for the cut due to the edge of the CCD): the pixel with the highest slope is then the value of x in which the derivative $\partial I(x)/\partial x$, reaches its maximum (see Fig. 4(below)). In order to find with better accuracy the position of the edge within the pixel, this one and the two pixels at its sides are fitted with a parabola.
We have made extensive tests in laboratory with illumination conditions similar to the one experienced during the run and we can say that the vertex of the parabola allows one to determine the position of the edge with a repeatability of approximately 0.07 arcsecs.

Every edge, obtained at a time t, is then represented by a vector of 192 elements, $[x_{(1,t)}, \ldots, x_{(192,t)}]_i$, with $i = 1, \ldots, s$, and every frame containing s images is reduceded to a matrix of s rows, each row corresponding to an edge.

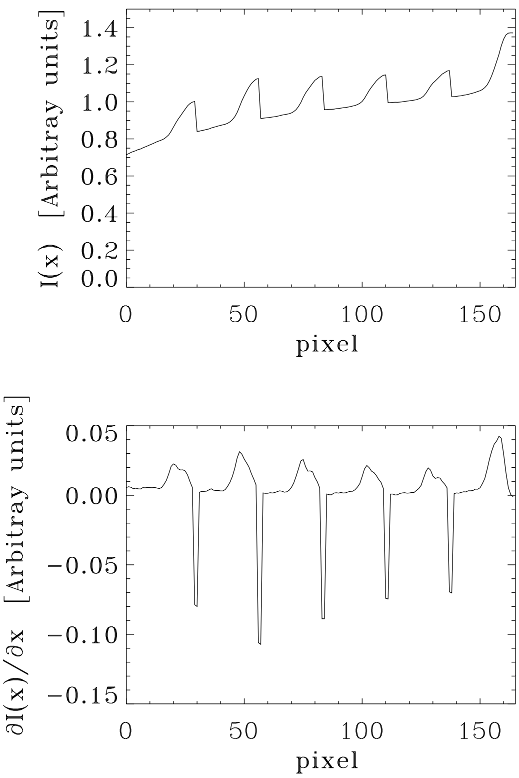

Fig. 4. Intensity plot in arbitrary units (above) and its derivative (below) along one column of the CCD

Rows of the same matrix are scaled in order to have the same value in the first element, that is equivalent to say:

$$x_{(1,t)_1} = \cdots = x_{(1,t)_i} = \cdots = x_{(1,t)_s}. \tag{3}$$

The standard deviation between the s rows, column by column, is then calculated moving along the edge, for $j = 1, \ldots, 192$:

$$\sigma_j = \sqrt{\frac{1}{s} \sum_{i=1\ldots s} \left(x_{(j,t)_i} - \bar{x}_{(j,t)}\right)^2}, \tag{4}$$

and this is equivalent to measuring the loss of correlation in the atmospheric induced tilt perturbations as the distance from a reference point increases.

Forcing all the edges in the same image to have the same value in the first pixel, introduces a multiplicative factor, $\sqrt{2}$, that has to be considered when determining the value of σ_j. The multiplicative factor arises because the variance of the first pixel, σ_1^2, sums quadratically with the absolute variance of each other pixel, $\sigma_{\rm abs}^2$, that is equivalent to say:

$$\sqrt{\sigma_1^2 + \sigma_{\rm abs}^2} = \sqrt{2\sigma_{\rm rel}^2}\,. \tag{5}$$

Plotting the standard deviation versus the distance from the reference position this loss of correlation is clearly visible (see Fig. 5). In these examples, over a distance of the order of less than 5 arcsec, the correlation is completely lost and the data show statistical oscillations

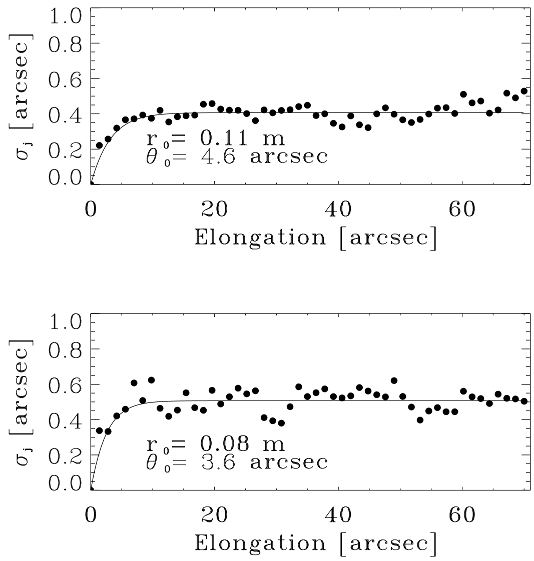

Fig. 5. Interpolating the data allows to obtain both the values for θ_0 and for r_0. It can be seen the loss of correlation between tilt perturbations for increasing distances from a reference point along the edge of the Moon. These are two examples of the data collected during the tests. Only one portion of the field of view, the most interesting, is plotted

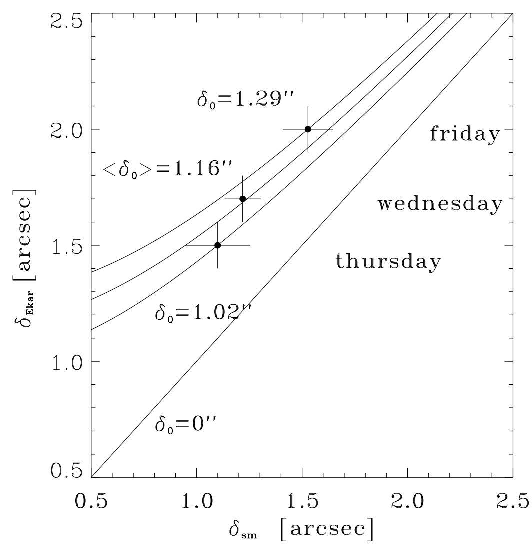

Fig. 6. The seeing measured at the Echelle spectrograph of Cima Ekar during the nights of the test is compared to the results obtained with the seeing monitor. The difference observed can be ascribed to dome seeing

around a mean value, σ_θ. This residual scatter is due both to Poissonian statistic, because of the limited number of edges collected in each image, to the photometric noise (including read out and photon shot noise) and finally to inhomogeneities in sensitivity of the pixels.

In order to find the value of θ_0, that is the value for which the correlation decreases of a factor e^{-1}, we fitted the data with the following function:

$$f(\theta) = \sqrt{2}\sigma_\theta \left[1 - \exp\left(-\frac{\theta}{\theta_0}\right)\right]. \quad (6)$$

However, it can be noted from one of the data plots, that this is only a rough approximation of the expected theoretical behaviour (Valley & Wandzura 1979).

In fact, sometimes one can observe at moderate angular distances an anticorrelation between the tilt perturbations and this is due to the fact that what is measured is not just the tilt component but instead it is the sum of both tilt and coma of any order.

Although we did not measure the anticorrelation because we had not enough samples to obtain a reliable estimate, it must be noted that knowing the amount of anticorrelation can be used to have a comparison between the observed turbulence power spectrum and that of Kolmogorov.

When the anamorphic relay is used to increase the size of the field of view it is possible, in principle, to increase the precision in the measurement of θ_0 within the same image. In fact one can choose to have as a reference point not only one of the pixels at the edges of the CCD but also one or more pixels in the center of the field, more distant from each other than the isokinetic angle.

Finally, considering the observed tilt effect on the rigid movement of the elongate LGS to be of the same order of that introduced in Eq. (1) one can recover (with the same equation but changing D_p from the diameter of the laser projector to the diameter of the seeing monitor) the characteristic value of r_0 for the night during which the tests where performed.

4. Results of the first experimental run

This seeing monitor has been tested on the nights of January 15, 16 and 17 at the Astrophysical Observatory of Asiago. During the same night, the images of the edge of the Moon where collected in two or more runs, separated by an amount of time greater than the typical e–folding time of the atmospheric perturbations (Racine 1996).
The results obtained from the collected data are summarized in Table 2.

As previously explained with this experiment one can simultaneously get both the value of the isokinetic angle, θ_0 (in the third column) and of the Fried parameter, r_0, (fourth column) but the latter is not measured directly.
It is then possible, with the following equation, to recover from r_0 the value of the seeing, here and in the following denoted as δ_sm, during the night of test (last column):

$$\delta_\mathrm{sm} \approx 206265 \left(\frac{\lambda}{r_0}\right) \quad \text{[arcsec]}, \quad (7)$$

It has not been possible to compare the results of the experiment with other seeing monitors. Nevertheless, during the same nights, astronomers at the Cima Ekar Telescope in Asiago gave an estimate to the seeing from the FWHM of the lines of the Echelle Spectrograph along the spatial scale. A comparison with their estimates (Fig. 6) shows consistency of the data obtained with this experiment, provided that one sums quadratically a blurring effect δ_0 to the seeing measured with our seeing monitor, δ_sm:

$$\delta_\mathrm{ekar} = \sqrt{\delta_0^2 + \delta_\mathrm{sm}^2}. \quad (8)$$

The blurring term, δ_0, includes both the effects of dome seeing, of jittering and tracking and of the optical aberrations of the 1.82 m telescope. Unfortunatly we could not measure directly r_0 with our seeing monitor and this is the only way we had to compare our results with an independent estimation.

A further relation has been searched using the data collected during the experiment. We said that one can partially ascribe to dome seeing and to errors introduced by the telescope the difference observed between the seeing monitor and the Cima Ekar telescope. The mean thermal gradient between the inside and the outside of the dome at Cima Ekar, measured during the three nights of the test, when compared to the difference in the seeing, δ_0, approximatively follows a law of this kind:

$$\delta_0 \approx 0.25 \Delta T. \quad (9)$$

With three available points, one for each night, it is only possible to show the proportionality between ΔT and δ_0: a comparison with other "seeing/temperature" relations, as reported for example by Lowne (1979) and by Bridgeland & Jenkins (1997), shows that the data collected with this experiment may fall in the range of values given by those authors.

Table 2. Measured values for the isokinetic patch and for the Fried parameter during the three nights of the test. The last two columns represent mean values for the same night

night	UT	θ_0''	$r_0 \pm \delta_{r_0}$[cm]	$\tilde{h}$[m]	$\bar{\delta}_\mathrm{sm}''$
15	19.40	4.0	9.4 ± 2.1	3350	1.2 ± 0.1
15	20.45	3.4	7.7 ± 0.8		
16	17.15	2.4	8.2 ± 1.7		
16	17.45	2.9	7.2 ± 1.2		
16	18.20	3.5	14.2 ± 2.5	3750	1.1 ± 0.3
16	19.20	4.6	10.5 ± 2.1		
17	17.50	3.2	6.6 ± 1.0		
17	18.30	3.6	8.1 ± 0.9	4100	1.5 ± 0.2
17	19.10	2.4	5.9 ± 0.9		

5. Conclusions

Knowing the size of the isokinetic patch can become important for some of the new techniques proposed to solve the tilt problem. Furthermore, the same perturbations observed in an elongated LGS can be easily seen observing the edge of the Moon. In this experiment several images of the edge of the Moon have been obtained with an optical system able to evaluate both the size of the isokinetic patch and r_0. A further run of the described instrument at the Telescopio Nazionale Galileo's (TNG) site in Canary islands (Barbieri 1997) could be very interesting to tune one's expectations about the effective performances of the Adaptive Optics module (Ragazzoni & Bonaccini 1995; Ragazzoni et al. 1997) which is actually under construction and will be permanently mounted at the Nasmith focus of the TNG.

Acknowledgements. Special thanks are due to Enzo Bellettato, Jacopo Farinato and to Marina Rejkuba for their helpful contribute during the observations and for the realization of the instrumentation described in the paper.

References

Acton D.S., 1995, Appl. Opt. 34, 4526
Barbieri C., 1997, SPIE Proc. 2871, 244
Belen'kii M.S., 1994, SPIE Proc. 2201, 321
Belen'kii M.S., 1995, SPIE Proc. 2471, 289
Belen'kii M.S., 1996, SPIE Proc. 2828, 280
Bridgeland M.T., Jenkins C.R., 1997, MNRAS 287, 87
Christou J.C., Ellerbroek B., Fugate R.Q., Bonaccini D., Stanga R., 1995, ApJ 450, 369
Foy R., Labeyrie A., 1985, A&A 152, L29
Foy R., Boucher Y., Fleury B., Grynberg G., McCullogh P.R., Migus A., Tallon M., 1992, ESO Conf. 42, 437
Foy R., Migus A., Biraben F., Grynberg G., McCullogh P.R., Tallon M., 1995, A&AS 111, 569
Kallistratova M.A., 1966, Radiophis. Quantum. Electron. 9, 50
Laikin M., 1973, Lens Design. Second edition, Dekker M. (ed.) Inc., New York
Lowne C.M., 1979, MNRAS 188, 249
McAlister H.A., 1976, ApJ 215, 159
McClure R.D., Arnoud J., Fletcher J.M., Nieto J.-L., 1991, Racine R., PASP 103, 370
Noll R.J., 1976, JOSA 66, 3
Olivier S.S., Max C.E., Gavel D.T., Brase J.M., 1993, ApJ 407, 428
Pilkington J.D.H., 1987, Nat 330, 116
Racine R., 1996, PASP 108, 372
Ragazzoni R., Bonaccini D., 1995, OSA Techn. Digest Ser. 23, 10
Ragazzoni R., Esposito S., Marchetti E., 1995, MNRAS, 276, L76
Ragazzoni R., Marchetti E., 1996, SPIE Proc. 2871, 948
Ragazzoni R., 1996a, A&A 305, L13
Ragazzoni R., 1996b, ApJ 465, L73
Ragazzoni R., 1997, A&A 319, L9
Ragazzoni R., Baruffolo A., Bortoletto F., D'Alessandro M., Farinato J., Ghedina A., Marchetti E., 1997, SPIE 2871, 905
Rigaut F., Gendron E., 1992, A&A 261, 677
Sivaramakrishnan A., Weymann R.J., Beletic J.W., 1995, AJ 110, 430
Tallon M., Foy R., 1990, A&A 235, 549
Valley G.C., Wandzura S.M., 1979, JOSA 69, 712
Weigelt G.P., 1979, Opt. Acta 26, 1351